Kinetic Characterization of the Function of Myosin Loop 4 in the Actin−Myosin Interaction†

Máté Gyimesi,‡ Andrey K. Tsaturyan,§ Miklós S. Z. Kellermayer,|| and András Málnási-Csizmadia*,‡

Department of Biochemistry, Eötvös University, Institute of Biology, Budapest, H-1117, Hungary, Institute of Mechanics, Lomonosov Moscow State University, Vorobjovy Gory, Moscow 119192, Russia, and Department of Biophysics, University of Pécs, Faculty of Medicine, Pécs, H-7624 Hungary

Received August 3, 2007; Revised Manuscript Received September 7, 2007

ABSTRACT: Myosin interacts with actin during its enzymatic cycle, and actin stimulates myosin's ATPase activity. There are extensive interaction surfaces on both actin and myosin. Several surface loops of myosin play different roles in actomyosin interaction. However, the functional role of loop 4 in actin binding is still ambiguous. We explored the role of loop 4 by either mutating its conserved acidic group, Glu-365, to Gln (E365Q), or by replacing the entire loop with three glycines (ΔAL) in a *Dictyostelium discoideum* myosin II motor domain (MD) containing a single tryptophan residue. This native tryptophan (Trp-501) is located in the relay loop and is sensitive to nucleotide binding and lever-arm movement. Fluorescence and fast kinetic measurements showed that the mutations in loop 4 do not alter the enzymatic steps of the ATPase cycle in the absence of actin. By contrast, actin binding was significantly weakened in the absence and presence of ADP and ATP in both mutants. Because the strength of actin−myosin interaction increases in the order of rigor, ADP, and ATP complex, we conclude that loop 4 is a functional actin-binding region that stabilizes actomyosin complex, particularly in weak actin-binding states.

Myosins are molecular motors that move along filamentous actin by converting the chemical energy of ATP[1] hydrolysis into mechanical work. Upon ATP binding myosin dissociates from F-actin, and ATP hydrolysis occurs when actin is mainly detached. Product release, actin rebinding, and force generation are kinetically coupled processes. According to the three-state docking model of myosin to actin (*1*) the formation of the collision complex is highly ionic-strength dependent, confirming that electrostatic interactions play an essential role in actin binding (*2*−*4*). High-resolution X-ray crystallography data revealed the presence of several surface loops in myosin's actin-binding region, which contain numerous charged residues.

Recently it was suggested that loop 4 of myosin may function as an actin-binding region or possess a regulatory role in actin binding (myosin 1b) (*5*). *Dictyostelium* loop 4 is an eight-residue surface loop in the upper 50 kDa subdomain of myosin near the cardiomyopathy loop (Figure 1). Loop 4 is also called cardiac loop (C-loop), because the role of this loop was investigated earlier on cardiac myosin as discussed below. The sequence of this loop is not significantly conserved among myosins, but there are some characteristic features. The basis of loop 4 is a conserved phenylalanine (Phe-359 in *Dictyostelium*) (Table 1) and most

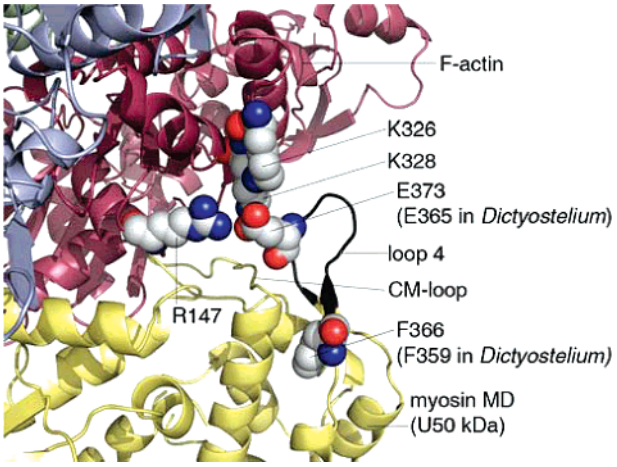

FIGURE 1: Simulated structure of the actomyosin interaction surface. A part of the actin−myosin interface in the model complex obtained by fitting chicken myosin II MD into cryo-EM electron density map of actomyosin complex (*13*). Actin monomers are shown in purple, light blue and light green, myosin MD is yellow and loop 4 is black. The basic amino acids (Lys-326, Lys-328 and Arg-147) of actin form a salt bridge cluster with Glu-373 (Glu-365 in *Dictyostelium* myosin II) of loop 4. Phe-366 (Phe-359 in *Dictyostelium* myosin II) stabilizes the cardiomyopathy loop (CM-loop), loop 4 and the N-terminal of the long Val^{419}−Gln^{448} (Asn^{410}−Cys^{442} *Dictyostelium* myosin II) α-helix which spans along the 50 kDa myosin subdomain. Phe-366, Lys-326, Lys-328 and Arg-147 are shown in spheres and colored as follows: carbon atoms are gray, oxygen atoms are red and nitrogen atoms are blue.

† This work was supported by National Office for Research and Technology RET 14/2005, OTKA TS49812, and Bolyai Fellowship sponsored by the Hungarian Academy of Sciences.

* To whom all correspondence should be addressed: Department of Biochemistry, Eötvös University, Institute of Biology, Budapest, H-1117, Hungary. Tel: +36-1-209-0555/8780. Fax: +36-1-381-2172. E-mail: malna@elte.hu.

‡ Department of Biochemistry, Eötvös University, Institute of Biology.

§ Institute of Mechanics, Lomonosov Moscow State University.

|| Department of Biophysics, University of Pécs, Faculty of Medicine.

[1] Abbreviations: ATP, adenosine 5′-triphosphate; ADP, adenosine 5′-diphosphate; MD, motor domain; M, myosin; A, actin; F-actin, filamentous actin; PyA, pyrene labeled F-actin; SEM, standard error of the mean.

10.1021/bi701554a CCC: $40.75
Published on Web 12/08/2007

Scheme 1

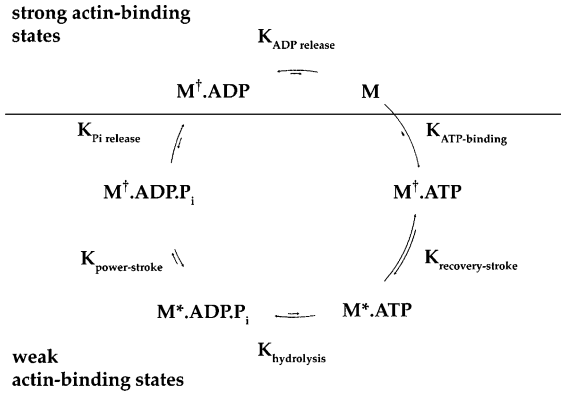

of the myosins contain negatively charged residue(s) in loop 4. So far it is not clarified whether loop 4 is a truly functional actin binding site, or it only stabilizes the actomyosin complex when already formed. Ajtai et al. showed that proteolytic cleavage of loop 4 in cardiac myosin S1 affects its actin-activated ATPase activity and sliding velocity, and actin protects loop 4 from limited tryptic proteolysis (*6*, *7*). However, the functional role of loop 4 in actomyosin complex formation remained ambiguous. Geeves et al. pointed out that loop 4, in their atomic model of the complex formed by myosin II and F-actin (*8*), does not seem to make contact with actin. By contrast, Coureux et al. (*9*) mentioned loop 4 as a previously uninvestigated loop in a position that enables interaction with actin. Furthermore, Holmes et al. (*10*) fitted the crystal structure of myosin V motor domain (MD) to cryo-EM density map of rigor actin−myosin V complex and suggested that loop 4 may become part of the binding site. The dynamic docking of myosin and actin carried out by Root et al. (*11*) suggests that loop 4 may interact with the N-terminus and the AA 90−100 region of actin. Flexible computer docking of myosin V apo-MD to F-actin (*12*) suggests that loop 4 is essentially involved in strong actin binding via both electrostatic and hydrophobic interactions. The docking of myosin V MD to actin (*12*) and fitting of myosin II structure into cryo-EM electron density map of the actomyosin complex performed by Holmes et al. (*13*) (Figure 1) suggest that the conserved Glu-365 (*Dictyostelium* numbering) is likely to be in a salt-bridge cluster with actin's Lys-326, Lys-328, and Arg-147.

In the present work we engineered three mutations in a *Dictyostelium* myosin II MD construct containing a single tryptophan at position 501 (W501+). In earlier studies it was demonstrated that this native relay-loop tryptophan at the 501 position (*Dictyostelium* numbering) senses the large conformational change of MD (*14*, *15*). This large conformational change involves the open−closed transition of switch 2 loop and the parallel movement of the lever-arm.

Scheme 1 is the extended form (*14*, *15*) of the classic Bagshaw−Trentham scheme (*16*), where low fluorescent $M^{\dagger}$ and high fluorescent M* states represent the open and closed switch 2 conformations, respectively. The fast ATP binding is followed by the open−closed transition, which is the recovery-stroke of myosin to develop the primed pre-hydrolysis M*.ATP state. Recovery-stroke is kinetically coupled to but distinct from the hydrolysis step which results in the posthydrolysis M*.ADP.P_i state. This high fluorescent state predominates the steady-state ATPase cycle of myosin II in the absence of actin. It is followed by the coupled isomerization and phosphate release steps, which are activated by actin. Apo and M.ADP states are strong actin binding states, while the other states possess weak acting binding properties in myosin II.

Table 1: Sequence Alignment of Loop 4[a]

Cardiac:	^{361}**G**	**N**	M	K	**F**	K	L	K	Q	R	E	-	*E*	Q	**A**	E^{375}
Skeletal:	^{363}**G**	**N**	M	K	**F**	K	Q	K	Q	R	E	-	*E*	Q	**A**	E^{377}
Smooth:	^{362}**G**	**N**	I	V	**F**	K	K	E	-	R	N	T	*D*	Q	**A**	S^{376}
Dicty:	^{355}**G**	**N**	I	K	**F**	E	K	G	-	-	A	G	*E*	G	**A**	V^{368}

[a] Alignment of loop 4 in human cardiac alpha myosin II, rabbit skeletal muscle myosin II, chicken gizzard smooth muscle myosin II and *Dictyostelium discoideum* myosin II. Residues in bold are identical in all of the four myosin isoforms. The acidic residues at position 365 (in *Dictyostelium* sp.) (italic) are conserved in all myosin classes except for the fission yeast myosin II (*Schizosaccharomyces pombe*) (*24*).

Since W501+ was shown to possess practically the wild-type phenotype, W501+ served as the basis of our mutants. All of the mutations presented in this work were introduced into the W501+ background, which enabled us to characterize their basic kinetic parameters and compare them with those of the W501+. To elucidate the role of the aromatic residue at the basis of loop 4, we designed the F359A mutation. To investigate the effects of the conserved negative charge at position 365, an E365Q mutation was introduced. In order to reveal the overall importance of loop 4, we replaced the entire loop (Lys^{361}−Val^{368}) with three glycine residues (ΔAL). Since loop 4 is structurally separate from other structural elements of myosin, its deletion is expected to result in a specific effect without disturbing the stability of neighboring regions. F359A, E365Q, and ΔAL mutants were analyzed by transient kinetic and fluorescence spectroscopic experiments. The results suggest that loop 4 is a functional actin-binding site that has an important role in the stabilization of the acto−myosin complex and has more pronounced role in weak actin-binding states.

EXPERIMENTAL PROCEDURES

All reagents were purchased from Sigma Chemical Co. All nucleotides and iodoacetamido-pyrene were purchased from Roche Co. Except where noted, the measurements were carried out using the following buffer: 20 mM Hepes, pH 7.2, 40 mM NaCl, 1 mM $MgCl_2$, 3 μM β-mercaptoethanol, 5 mM benzamidine-HCl, 20 °C (assay buffer).

Protein Engineering. Our constructs are based on the W501+ *Dictyostelium discoideum* myosin II MD of the M761 construct described in (*14*). We applied mutant PCR oligonucleotide primers to introduce the codons of glutamine or alanine or three glycines into the W501+ construct. As a template, pDXA-3H/W501+ construct was used and the following primers: GGT AAC ATC AAA *TTC GAA* AAA GGT GCT GGT CAA GGT GC for E365Q, GGT AAC ATC AAA GCA GAA AAA GGT GCT GGT CAA GGT GC for F359A, and GGT AAC ATC AAA *TTC GAA* GGT GGT GGT CTC AAA GAC AAA ACC GCC for ΔAL (mutated positions underlined). In all cases the downstream primer

was an MD-specific oligonucleotide that resulted in a 729-base-pair product, from which *Bsp*119I (restriction site is italicized in the primer sequences) digestion cut out a 321-bp fragment. Since F359A mutation affects the *Bsp*119I restriction site, in this case we applied a megaprimer method in which the first PCR product serves as the primer for the second PCR reaction. Here we digested the second PCR product with *Eco*72I and *Bsp*119I. Fragments were then ligated into a pGEM-11Zf(+)/W501+ construct that had also been digested with *Bsp*119I or *Eco*72I/*Bsp*119I. The orientations of the inserts and the mutations were verified by sequencing. The correct clones were subcloned into pDXA-3H vector using *Bam*HI sites. Here, orientation was tested by *Bgl*II digestion. The final amino acid sequences of loop 4 segments of E365Q, F359A, and ΔAL constructs were ^{359}-FEKGAGQGAVL^{369}, ^{359}AEKGAGEGAVL^{369}, and ^{359}-FEGGGL^{369}, respectively (mutations underlined).

Expression and Purification of Proteins. Dictyostelium cells were grown and plasmids electroporated as described earlier (*17*). Protein purification was carried out as described previously (*14*). Actin was purified according to established protocols (*18*, *19*). Pyrene labeling of actin was carried out as in (*20*).

Steady-State Fluorescence. Steady-state spectra and time courses were detected in a FluoroMax SPEX-320 spectrofluorimeter at 20 °C. Excitation wavelength was 296 nm, which enabled us to excite tryptophans specifically without exciting tyrosines. Slits were 2 nm on both the excitation and the emission monochromators. Emission spectra were recorded from 305 to 420 nm to avoid detecting direct light. We used a Hellma 105.250-QS precision cuvette with 10 mm path length. Time courses were recorded with the same settings on the excitation side, and the emission monochromator was adjusted to 340 nm where the intensity changes of W501 fluorescence were maximal.

Transient Kinetics. Transient kinetic measurements were carried out using either a KinTek-2004 stopped-flow apparatus that has a 1 ms dead time at the applied 15-mL/s flow rate (*21*) or a BioLogic SFM-300/400 stopped-flow instrument. Temperature was kept constant at 20 °C with a water circulator. Tryptophan fluorescence was measured with 2 nm slit width at an excitation wavelength of 297 nm to select the intensity peak of the mercury−xenon lamp used (Hamamatsu Super-Quiet Mercury Xenon Lamp). At the emission side a 340 nm interference filter was applied (Corion CFS-001999 9L134) which has negligible self-fluorescence compared to cutoff filters (*22*). Pyrene fluorescence was measured with 4 nm slit width at an excitation wavelength of 280 nm, and FRET emission was detected through a 390 nm cutoff filter on the emission side, or 365 nm excitation wavelength was combined with a 420 nm cutoff filter. Light scattering measurements were carried out by using the 340 interference filter, and the monochromator was set to 340 nm with 4 nm slit width at the excitation side.

Actin-Activated ATPase Measurement. Actin-activated ATPase activity was determined with a pyruvate kinase/lactate dehydrogenase coupled assay at 20 °C as described in (*23*). Buffer conditions were 5 mM Hepes, pH 7.2, 1 mM $MgCl_2$ and 1 mM KCl. The concentration of the MD constructs was 0.5 μM, and actin concentration varied between 0 and 150 μM.

Acto−MD Cosedimentation. All samples were made in assay buffer at room temperature, and myosin MD was added to the mixtures on ice right before starting the ultracentrifugation. Ultracentrifugation was carried out with a Beckman Optima TL Ultracentrifuge and the Beckman TLA 100.1 rotor operated for 15 min at 4 °C and 228000*g*. 100 μL of the total 200 μL supernatants and pellets resuspended in 100 μL of assay buffer were run on 4−20% Tris-Glycine Gel (Invitrogen Co.) and were analyzed by using GeneSnap and Gene Tools from SynGene softwares.

RESULTS

The kinetic parameters of W501+ construct have been determined in detail in (*14*, *15*) and showed the same properties as those of wild type MD. Trp-501 is highly sensitive for nucleotide binding and the recovery stroke step coupled with hydrolysis, therefore the measurement of fluorescence signal change upon nucleotide binding allow us to determine the kinetic properties of these reaction steps. The advantage of W501+ over the wild type MD is that the signal change is much larger in the single tryptophan MD construct than in the wild type which have three other nonresponding tryptophans. We exploit in this advantage by constructing loop 4 mutation constructs with the W501+ backgrounds. Each measurement of this study was also carried out on W501+, which served as a control for the observed effects of the mutants. E365Q mutation was introduced into the tip of loop 4 to eliminate the charge from the proposed salt bridge between actin and myosin. ΔAL was prepared to investigate the role of the entire loop, therefore the sequence of the wild-type loop was replaced with 3 glycines. F359A mutation was designed for testing the role of this aromatic residue at the base of loop 4 which is highly conserved among myosins (*24*). The protein expression levels of E365Q and ΔAL were similar to those of W501+ and wild type MD (approximately 10 mg/L *Dictyostelium* culture), while for F359A it decreased by one order of magnitude.

Steady-State ATPase Activities of E365Q, ΔAL, F359A, and W501+. The steady-state ATPase activities of E365Q and ΔAL were similar to those of W501+ and wild type MD (0.05 s^{-1}), while F359A did not hydrolyze ATP.

Enzymatic Activities of F359A Mutant. The steady-state fluorescence spectrum of F359A showed a 14% fluorescence decrease with 1 nm blue shift upon adding ATP. A similar effect was obtained when 1 mM ADP was added as the fluorescence intensity decreased by 11% and a small blue shift was detected. By contrast, W501+ shows 80% fluorescence increase and 15% decrease upon adding ATP and ADP, respectively. Fluorescence decrease of Trp-501 corresponds to nucleotide binding, while fluorescence increase occurs during the large conformational change (recovery stroke step) coupled with the hydrolysis step (*15*). When F-actin was mixed with F359A, the light scattering increased as much as it occurred in the cases of W501+, which indicates that the mutant binds F-actin. However, upon adding ATP the light scattering did not drop as much as for W501+, and reattachment was not detected either, suggesting that ATP was not consumed by F359A also in the presence of actin. These results demonstrate that F359A is able to bind nucleotides and actin, but ATP-induced actin dissocia-

Table 2: Kinetic Parameters of the Acto−Myosin Interaction in the Absence and in the Presence of ADP

	k_{-D} (s^{-1})	k_{+D} (μM^{-1} s^{-1})	$K_{d,D}$ (μM)	k_{-A} (s^{-1})	k_{+A} (μM^{-1} s^{-1})	$K_{d,A}$ (μM)	k_{-DA} (s^{-1})	k_{+DA} (μM^{-1} s^{-1})	$K_{d,DA}$ (μM)	$K_{d,AD}$ (μM)
W501+	8.2 ± 0.071	1.2 ± 0.033	7.1	0.047 ± 0.0020	1.6 ± 0.044	0.030	0.027 ± 0.0021	0.22 ± 0.016	0.12	33 ± 1.1
E365Q	9.8 ± 0.15	2.0 ± 0.023	5.0	0.057 ± 0.0019	1.6 ± 0.039	0.036	0.049 ± 0.0020	0.17 ± 0.0075	0.30	50 ± 2.4
ΔAL	14 ± 0.21	1.5 ± 0.043	9.3	0.087 ± 0.0060	1.4 ± 0.026	0.064	0.077 ± 0.0039	0.18 ± 0.0086	0.43	37 ± 1.1

Scheme 2

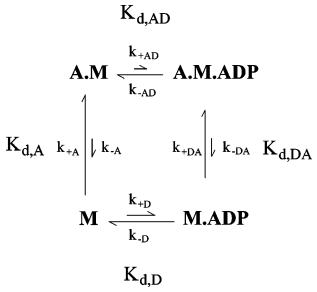

tion is partially blocked. In addition, F359A does not consume ATP either in the presence or in the absence of actin because of inhibition of the recovery stroke step (open−closed transition of switch 2 loop (*15*)).

Steady-State Fluorimetric Properties of E365Q and ΔAL. According to (*14*), in the presence of 1 mM ATP, W501+ is fully saturated and shows 80% fluorescence enhancement coupled with a 6 nm blue-shift. Upon addition of ATP, both E365Q and ΔAL showed the same 6 nm blue shift, and 85% and 75% fluorescence intensity enhancement, respectively. In the presence of 1 mM ADP the fluorescence intensity of all constructs decreased by 10−20%, and the blue shifts were 2−5 nm. In summary, these results demonstrate that in the absence of actin all steady-state fluorescence properties of both loop 4 mutants are very similar to those of W501+.

Kinetic Characterization of E365Q and ΔAL in the Absence of Actin. The ATP-induced fluorescence change reflects the recovery stroke step that occurs mainly in the relay region and in the switch 2 loop coupled with the hydrolysis step. 3 μM MD samples were mixed with ATP at 5−500 μM (if otherwise not stated, the concentrations are postmix values), and fluorescence increase was followed. Data were fitted best to a hyperbola ($k_{obs} = k_{max}[ATP]/([ATP] + K_{0.5})$), and both E365Q and ΔAL yielded practically the same maximum rate constants of 39 and 38 s^{-1}, respectively. These values are similar to that of W501+ (35 s^{-1}) at 20 °C. In order to characterize ADP binding processes by stopped flow, MD samples were rapidly mixed with 5−200 μM ADP, and the fluorescence quench was followed. The rate constants of binding and release of ADP were only slightly altered by the mutations and fit well to the previously published data on W501+ (see Scheme 2 and Table 2) (*14*). These findings confirm the assumption that, in the absence of actin, both mutants possess the wild type phenotype, therefore neither mutation perturbs the basic kinetic characteristics.

ATP-Induced Actomyosin Dissociation of E365Q and ΔAL. Transient kinetic measurement of acto−myosin dissociation, followed by light scattering, showed significant difference between W501+ and the mutants (Figure 2). Mixtures of 3 μM F-actin stabilized with 3 μM phalloidin were preincubated with 2.5 μM MD samples. This solution was mixed with 0.02−5 mM ATP in the stopped flow, and light scattering change due to acto−myosin dissociation was followed. The observed rate constants were plotted against ATP concentration, and hyperbolas were fitted. The maximum rate constant of W501+ was $k_{max;W501+} = 117 \pm 2.2$ s^{-1} (standard error of the mean (SEM) is presented in all cases), and the initial slope of the hyperbola was $k_{on,ATP,W501+} = 0.15$ s^{-1} μM^{-1}, which reflects the second-order rate constant of ATP binding (K_1k_{+2} according to the Bagshaw−Trentham scheme equation 7 in (*16*)). Both mutations caused large increases in k_{max} ($k_{max;E365Q} = 260 \pm 5.2$ s^{-1} and $k_{max;\Delta AL} = 932 \pm 29$ s^{-1}), but the second-order rate constants of ATP binding were practically unchanged ($k_{on,ATP,E365Q} = 0.25$ s^{-1} μM^{-1} and $k_{on,ATP,\Delta AL} = 0.18$ s^{-1} μM^{-1}). These results indicate that loop 4 mutations affect acto−myosin interaction, but they do not significantly influence ATP binding.

ADP Inhibition of ATP-Induced Actin Dissociation of E365Q and ΔAL. ADP dependent inhibition of ATP induced actin−myosin dissociation determines the ADP affinity to the actomyosin complex. 0.5 μM W501+, E365Q, or ΔAL was premixed with 0.6 μM pyrene-labeled, phalloidin-stabilized F-actin in the absence or presence of varying amounts of ADP. This preincubated solution was rapidly mixed with 200 μM ATP (premix concentrations). Increase in pyrene fluorescence accompanying the dissociation reaction was followed, and single exponentials were fitted to the traces. The values of $k_{AM,off,ADP}/k_{AM,off}$ were plotted against ADP concentration, where $k_{AM,off,ADP}$ (k in Figure 3) is the observed rate constant of the reaction at the given ADP concentration and $k_{AM,off}$ (k_o in Figure 3) is the observed rate constant of the reaction in the absence of ADP. Hyperbolas were fitted to the plots, where ADP concentration at the half-maximal saturation reflects the dissociation constant of ADP for acto−MD complex ($K_{d,AD}$, Scheme 2). Both mutations caused a relatively small increase in $K_{d,AD}$ (Figure 3 and Table 2).

Acto−Myosin Association and Dissociation of E365Q and ΔAL in the Absence of Nucleotides. The role of loop 4 in the formation of the acto−myosin rigor complex was investigated by mixing 0.05 μM pyrene-labeled actin with 0.05−1.5 μM MD constructs in stopped-flow and following pyrene fluorescence changes upon the association reaction. The on-rate constants (k_{+A}) showed negligible differences between W501+ and the mutants (Table 2, Figure 4A). Actin dissociation was studied by chasing the bound pyrene-labeled F-actin with unlabeled F-actin. In these experiments 0.2 μM MD constructs were preincubated with 0.2 μM pyrene-labeled F-actin and mixed with 2 μM unlabeled F-actin in a stopped-flow apparatus. Single exponentials were fitted on the enhancing fluorescence traces (Figure 4C) that yielded the rate constant of actin dissociation (k_{-A}) (Table 2). In contrast to the on-rate constants, the mutations caused significant increase in the off-rate constant ($k_{-A;W501+} = 0.047$ s^{-1}, $k_{-A;E365Q} = 0.057$ s^{-1}, $k_{-A;\Delta AL} = 0.085$ s^{-1}) of actin dissociation in the absence of nucleotide.

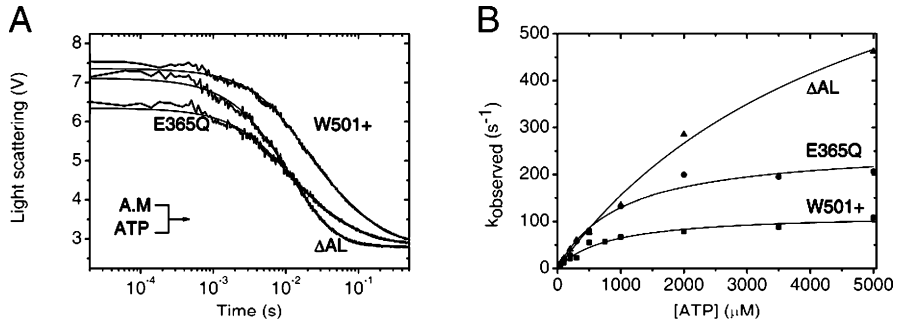

FIGURE 2: ATP-induced acto−myosin dissociation followed by light scattering. (A) Stopped-flow records on mixing 2.5 μM mutant MD preincubated with 3 μM phalloidin-stabilized F-actin with 1 mM ATP. The observed rate constants of actin dissociations of W501+, E365Q and ΔAL constructs were 69.59 s^{-1}, 118.6 s^{-1} and 150.8 s^{-1}, respectively. (B) ATP concentration dependence of the observed rate constants of ATP induced actin dissociations of the three constructs. Hyperbolas were fitted to the curves. V_{max} values increased due to the mutation (117 s^{-1} (W501+, ■), 260 s^{-1} (E365Q, ●) and 932 s^{-1} (ΔAL, ▲)) while the initial slopes did not change significantly (0.15 $s^{-1}\mu M^{-1}$ (W501+), 0.25 $s^{-1}\mu M^{-1}$ (E365Q), 0.18 $s^{-1}\mu M^{-1}$ (ΔAL)).

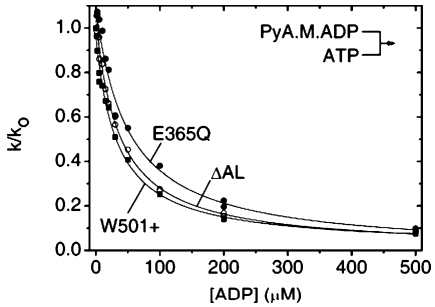

FIGURE 3: ADP inhibition of ATP induced actomyosin dissociation. 0.5 μM MD and 0.6 μM pyrene-labeled F-actin was preincubated in the absence or in the presence of different amounts of ADP and was mixed with 200 μM ATP in the stopped-flow (premix concentrations). Pyrene fluorescence signal was followed and single exponentials were fitted (k). According to the ADP concentration dependence of the k/k_o determines ADP affinity ($K_{d,AD}$) to the actomyosin complex, if k_o is the observed rate constant in the absence of ADP. Both mutants showed slightly increased $K_{d,AD}$ values ($K_{d,AD\ E365Q}$ = 50.0 μM (E365Q, ●) and $K_{d,AD\ \Delta AL}$ = 36.5 μM (ΔAL, ○)) compared to $K_{d,AD\ W501+}$ = 33.2 μM (W501+, ■).

Acto−Myosin Association and Dissociation of E365Q and ΔAL in the Presence of ADP. All settings and conditions were the same as in the previously described experiments, except for the addition of 1 mM ADP. Similarly to the rigor complex, the on-rate constants of acto.MD (k_{+DA}) did not vary significantly (Table 2, Figure 4B). By contrast, we found a greater increase in the off-rate constants (k_{-DA}) in the mutants in the presence of ADP ($k_{-DA;W501+}$ = 0.026 s^{-1}, $k_{-DA;E365Q}$ = 0.049 s^{-1}, $k_{-DA;\Delta AL}$ = 0.076 s^{-1}) compared to those in the absence of the nucleotide (Table 2, Figure 4D). The dissociation constant of acto−MD complexes increased more in the presence of ADP ($K_{d,DA}$, 3.6 times) than in the absence of ADP ($K_{d,A}$, 2.1 times) (Table 2).

Actin-Activated ATPase Activity of E365Q and ΔAL. Actin-activated ATPase activities were determined in the range of 0−150 μM actin concentration at low ionic strength (I = 3 mM). A hyperbola (activity = V_{max}[actin]/(K_m + [actin])) was fitted to the plot of the specific ATPase activity of W501+ on actin concentration at 0−105 μM (Figure 5). Above 110 μM of actin concentration the actin activated ATPase activity declines with increasing actin concentration because the ATP hydrolysis step becomes the rate-limiting reaction step as it was described by White et al. (*25*). The ATPase activity of W501+ saturated at $V_{max\ actin(W501+)}$ = 3.70 ± 0.061 s^{-1} and $K_{m\ actin(W501+)}$ = 19.9 ± 0.896 μM. The mutations caused large changes in the parameters of actin-activated ATPase activities, as $K_{m\ actin}$ values of E365Q and ΔAL increased by 5.9 and 8.5 times, respectively ($K_{m\ actin(E365Q)}$ = 117.6 ± 13.36 μM and $K_{m\ actin(\Delta AL)}$ = 169.9 ± 10.85 μM). On the other hand, only small changes were detected in maximal steady-state actin activated ATPase rate constants ($V_{max\ actin(E365Q)}$ = 3.54 ± 0.250 s^{-1} and $V_{max\ actin(\Delta AL)}$ = 3.46 ± 0.156 s^{-1}) as compared with W501+.

Fractional Binding of Acto−MD during Steady-State ATP Hydrolysis. To investigate the weak binding properties of myosin MD, 2 μM myosin MDs were mixed with different amounts (0−60 μM) of phalloidin stabilized F-actin in the presence of 5 mM ATP in order to fully saturate the MDs throughout the ultracentrifugation. Supernatants and pellets were run on acrylamide gel and Coomassie-stained bands were analyzed. Figure 6A and B show the fractional binding of the different MDs to actin. In the case of W501+ more than 50% was cosedimented at 60 μM actin concentration, while in the case of the mutants only around 25%. The difference between E365Q and ΔAL is negligible. Thus, both mutations weakened the actin-binding properties of the motor domain in the weak actin-binding state when saturating amount of ATP was presented. Control experiments show that all MD constructs bind actin strongly in the absence of ATP.

In summary, the results of the actin binding experiments in the absence and presence of ADP and ATP indicate that the weaker the actomyosin binding, the greater the effect of loop 4 mutations on actomyosin interaction.

DISCUSSION

In the present work we show that loop 4 of myosin II plays a functional role in the stabilization of the actomyosin complex through regulating the off-rate constant of acto−myosin interaction. In order to investigate the effects of loop 4 mutations on the actin binding properties we designed the mutations in the W501+ construct characterized in earlier studies (*14*, *15*). In these studies it was concluded that the kinetic parameters of W501+ do not differ from the wild type MD significantly. The single tryptophan background of W501+ in the mutant constructs enabled us to follow nucleotide binding and the recovery stroke steps directly through the intrinsic fluorescence signal. The kinetic parameters of loop 4 mutants were compared with those of W501+.

Actin and myosin have an extended interaction surface to which the myosin motor domain and at least two actin

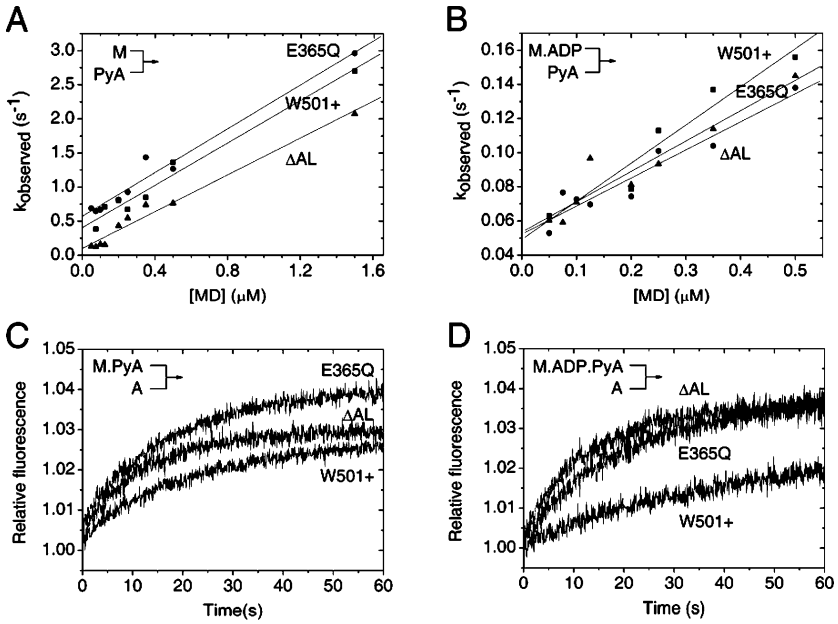

FIGURE 4: Actomyosin interaction in the absence and presence of ADP. (A, B) Determination of the on-rate constants: the observed rate contants of actomyosin association measured by stopped-flow experiments are plotted against MD concentrations in the absence (A) and presence of ADP (B). 0.05 μM pyrene-labeled F-actin was mixed with 0.05−1.5 μM MD in stopped-flow, and pyrene fluorescence was followed. (C, D) Determination of the off-rate constants with chase reactions. 0.2 μM pyrene-labeled actin was preincubated with 0.2 μM myosin motor domain mutants and mixed with 2 μM F-actin in the absence (C) or in the presence of ADP (D) in stopped-flow and pyrene fluorescence was followed. The calculated values from the data shown here are presented in Table 2.

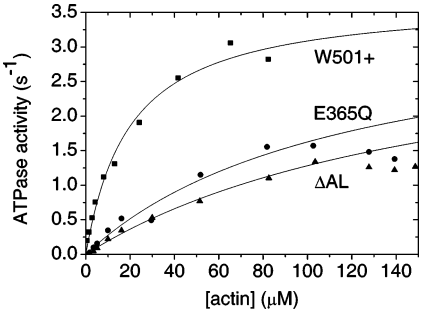

FIGURE 5: Actin-activated ATPase activity of W501+, E365Q and ΔAL. Actin activated ATPase activities were measured in a low-ionic-strength buffer (see Experimental Procedures). Hyperbola was fitted on the data, which determined the $V_{max\ actin}$ and $K_{m\ actin}$ values. Both mutations caused significant effect in both parameters. The $V_{max\ actin(W501+)}$ = 3.70 s^{-1} (■) was slightly decreased in the case of E365Q ($V_{max\ actin(E365Q)}$ = 3.54 s^{-1}, ●) and ΔAL ($V_{max\ actin(\Delta AL)}$ = 3.46 s^{-1}, ▲). However, $K_{m\ actin}$ values showed significant differences in both mutants compared to that of W501+: $K_{m\ actin(W501+)}$ = 19.89 μM, $K_{m\ actin(E365Q)}$ = 117.6 μM and $K_{m\ actin(\Delta AL)}$ = 169.9 μM.

monomers contribute. Since the high-resolution structure of the actomyosin complex is not available yet, we need to rely on the existing kinetic and docking data. X-ray crystallography, electron micrograph and computer docking studies (*12*, *13*) revealed several surface loops on myosin's actin-binding surface, many of which contain charged residues. There is a large body of kinetic evidence that emphasizes the importance of charged residues in the proximity of the actomyosin interface. These charge−charge interactions are supported by the N-terminus of actin subdomain 1, which also contains a large number of charged amino acid pairs that highly influence myosin activity. The actin-binding properties of myosin's surface loops and the myosin-binding properties of actin's N-terminal regions have been extensively explored (summarized in Supporting Information as Supplementary Table).

Loop 4 of myosin was also presumed to be a functional actin-binding element, but its specific role has not been investigated in detail. In a recent study (*5*), loop 4 of myosin Ib was demonstrated to play a modulatory role in acto−myosin interaction. Myosin Ib possesses a long loop 4 region that modulates actin binding in a tropomyosin-dependent manner. However, this effect was not observed when the loop 4 sequence of myosin Ib was replaced with that of the *Dictyostelium* sequence. Therefore, loop 4 presumably does not play this kind of role in our constructs, but highlights that loop 4 might be a modulatory region in myosins. Previously Ajtai at al (*7*) investigated the role of loop 4 in actin binding by mutagenesis analysis, where they introduced the R370E (smooth muscle numbering) mutation into smooth muscle myosin II heavy meromyosin (HMM). However, the relevance of this mutation is limited, because there is a low sequence similarity between loop 4 of cardiac myosin and smooth muscle myosin II (9 differences in the 16 residues), and neither of the two myosins were investigated by actomyosin docking experiments. The experiments using limited proteolysis were carried out on cardiac muscle myosin that shows high similarity with skeletal myosin II in this region (1 difference in the 16 residues). The mutations were designed based on the atomic structure of skeletal myosin II, while mutation was introduced into smooth muscle myosin II HMM. Based on actin docking studies of skeletal myosin II and myosin V, R370E of smooth muscle myosin might not have direct contact with actin residues. In addition, Arg-370 is not a conserved amino acid according to sequence alignments (*24*) (Table 1). By contrast, docking results (*12*, *13*) showed that loop 4 is in close proximity to actin surface loops connecting subdomain 1 and 3 of actin. In the docking models Glu-365 of *Dictyostelium*, or the equivalent Glu-373

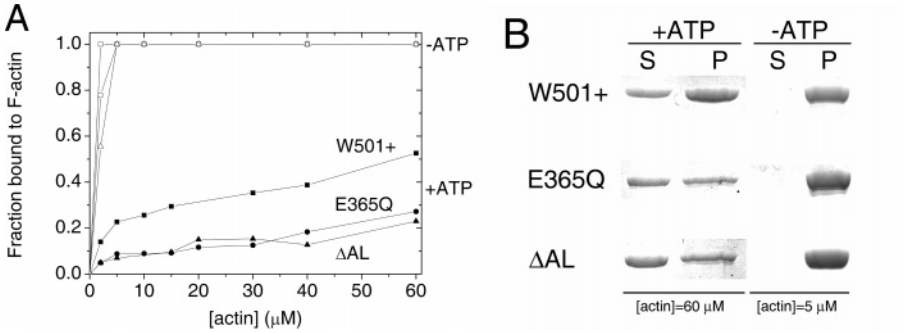

FIGURE 6: Cosedimentation of actin and MDs in the absence or in the presence of ATP. Actin binding of W501+ and the mutants in the absence and presence of 5 mM ATP. In these cosedimentation experiments 2 μM MDs were mixed with varying amount of F-actin. (A) This figure shows the fractional binding of W501+ (■ and □), E365Q (● and ○) and ΔAL (▲ and △) to F-actin as a function of actin concentration. Solid and open symbols represent data points in the presence and in the absence of ATP, respectively. In the absence of ATP all three constructs were 100% cosedimented with actin at [actin] ≥ 5 μM and only a slight difference can be detected at 2 μM actin concentration. In the presence of ATP 50% binding of W501+ to actin occurred at [actin] ≥ 60 μM, while the mutants showed approximately 25% binding at [actin] ≥ 60 μM. These data demonstrate weakened actin binding properties of the mutants. Furthermore, the negative charge at the tip of loop 4 plays an important role in actin binding as the effect of the charge elimination is in the order of the entire loop deletion. (B) The Coomassie-stained bands of supernatants (S) and pellets (P) of the MDs at the highest studied (60 μM) actin concentration in the presence of ATP; and at [actin] = 5 μM in the absence of ATP. In the presence of ATP more than 50% of W501+ is in the pellet (for parameters see Experimental Procedures), while in the case of E365Q and ΔAL the greater part was in the supernatant.

position in chicken skeletal myosin II, forms a complex salt-bridge with actin's Lys-328, Lys-326 and Arg-147 (Figure 1). Except for the fission yeast (*Schizosaccharomyces pombe*), myosin II all of the class II myosins contain acidic side chain in this position, and it is also conserved in most of the myosin classes (*24*).

Considering the prior implications we aimed to test the role of Glu-365 of myosin in the interaction between actin and myosin. Since replacement of Glu-365 with alanine would perturb the system more considerably, we engineered an E365Q mutation to specifically test the effect of the negative charge. The same strategy was applied by Giese and Spudich (*26*), who mutated the E531 of the H-loop-H region of *Dictyostelium* myosin into glutamine to investigate the role of the charged residue in actomyosin interaction. To elucidate the function of the entire loop in actin binding, we designed a construct, signed as ΔAL, in which loop 4 was deleted between positions Lys^{361}−Val^{368} and was substituted with three glycines. Note that loop 4 in *Dictyostelium discoideum* MD naturally contains 3 glycines, so this mutation is deletions of the neighboring amino acids. Neither the substitution of the entire loop with the three native glycines nor the single negative charge elimination by E365Q mutation affects any basic function of myosin motor domain in the absence of actin, implying a specific role of loop 4 in the acto−myosin interaction. This specific property is underlined by the fact that loop 4 is a structurally distinct loop.

We introduced another mutation at the base of loop 4 at position 359 (F359A). This highly conserved phenylalanine very likely stabilizes loop 4, the cardiomyopathy loop and the long helix (Asn^{410}−Cys^{442} in *Dictyostelium*, Val^{419}−Gln^{448} in chicken skeletal myosin) which spans the upper 50 kDa subdomain. This mutation caused the loss of ATPase activity as the steady-state fluorescence intensity in the presence of saturating ATP decreased with 14% similar to that observed with ADP (11%). This demonstrates a blocking of the conformational change of switch 2 loop of the nucleotide binding pocket. Since closed conformation of switch 2 is required for hydrolysis (*15*), F359A is unable to hydrolyze ATP. Further effect of this mutation is the weakened ability to dissociate from actin upon ATP binding. These results implicate a crucial role of this residue in the stabilization of the structure of several regions of MD, which elucidates the reason for its conservativity among different myosin classes.

E365Q and ΔAL showed weakened actin binding especially when nucleotide was bound to myosin's active site. Our kinetic data show the tendency that the weaker the acto−myosin interaction, the greater the weakening effect of loop 4 mutations on the actin binding of myosin. Loop 4 deletion caused only 2.1-fold increase in the actomyosin dissociation constant ($K_{d,A}$), while 3.6- and 8.5-fold increases were detected in the presence of ADP and ATP, respectively. In all cases, weakening of actin-binding properties is mainly due to increased off-rate constants (k_{-A} and k_{-DA}), while the actin binding on-rate constants (k_{+A} and k_{+DA}) are not changed by the mutations. It is confirmed by the 8-fold increase in the maximal observed rate constant (k_{max}) of the ATP induced actomyosin dissociation caused by loop 4 deletion. In all cases E365Q mutation caused intermediate effects between the wild type and ΔAL. These observations implicate that loop 4 plays a functional modulatory role in actomyosin interaction.

The value of $K_{m\ actin}$ of actin activated ATPase reflects the strength of actin binding in ATP. We found a 8.5-fold increase in $K_{m\ actin}$ of ΔAL, while the maximal actin activated ATPase activities ($V_{max\ actin}$) of the mutants were almost unaltered. Because of the very weak actin binding of the mutants we could not saturate myosin with actin and determine $V_{max\ actin}$ values precisely, which might be the reason for the small differences in $V_{max\ actin.}$

The significant weakening of actin binding in the presence of ATP was also demonstrated in the actomyosin cosedimentation experiments where actin and myosin are ultracentrifuged in the presence of saturating amount of ATP. These data showed that at high actin concentration (60 μM) 50% of the W501+ was cosedimented with actin despite the presence of ATP. By contrast, this value was only approximately 25% in the case of the mutants. This and the

actin activated ATPase experiments emphasize that loop 4 has significant functional role in actin binding especially in the weak actin binding states.

$K_{d,AD}$ values (Scheme 2) were only slightly changed and are consistent with the calculated parameters from the thermodynamic box in Scheme 2. We determined all kinetic parameters of the thermodynamic box experimentally (Table 2). ADP binding in the absence of actin remained practically unchanged, but $K_{d,AD}$ values in the presence of actin increase as many times as the coupling ratio of ADP binding in the absence and presence of actin $K_{d,D}/K_{d,AD}$ (*27*).

In summary, we conclude that loop 4 of myosin II is a functional actin binding region. It stabilizes actin−myosin interactions which role is more pronounced in the weak actin binding states than in rigor. Although the sequence of loop 4 is not conserved among different myosin classes (*24*), even between isoforms (Table 1), most of the known myosins have negatively charged residue(s) probably at the tip of loop 4 (Glu-365 in *Dictyostelium* myosin II) which form a salt bridge cluster with the positively charged residues of actin. Probably the strength of this salt bridge cluster regulates the stability of weak actin binding.

ACKNOWLEDGMENT

We thank Bálint Kintses for helpful comments and discussions.

SUPPORTING INFORMATION AVAILABLE

Summary of the effect of the mutations in the actomyosin interacting surface introduced into either myosin or actin mentioned as Supplementary Table. This material is available free of charge via the Internet at http://pubs.acs.org.

REFERENCES

1. Geeves, M. A., and Conibear, P. B. (1995) The role of three-state docking of myosin S1 with actin in force generation, *Biophys. J. 68*, 194S−199S.
2. Conibear, P. B. (1999) Kinetic studies on the effects of ADP and ionic strength on the interaction between myosin subfragment-1 and actin: implications for load-sensitivity and regulation of the crossbridge cycle, *J. Muscle Res. Cell Motil. 20*, 727−742.
3. Geeves, M. A., and Gutfreund, H. (1982) The use of pressure perturbations to investigate the interaction of rabbit muscle myosin subfragment 1 with actin in the presence of MgADP, *FEBS Lett. 140*, 11−15.
4. Geeves, M. A., and Jeffries, T. E. (1988) The effect of nucleotide upon a specific isomerization of actomyosin subfragment 1, *Biochem. J. 256*, 41−46.
5. Lieto-Trivedi, A., Dash, S., and Coluccio, L. M. (2007) Myosin surface loop 4 modulates inhibition of actomyosin 1b ATPase activity by tropomyosin, *Biochemistry 46*, 2779−2786.
6. Ajtai, K., Garamszegi, S. P., Park, S., Velazquez Dones, A. L., and Burghardt, T. P. (2001) Structural characterization of beta-cardiac myosin subfragment 1 in solution, *Biochemistry 40*, 12078−12093.
7. Ajtai, K., Garamszegi, S. P., Watanabe, S., Ikebe, M., and Burghardt, T. P. (2004) The myosin cardiac loop participates functionally in the actomyosin interaction, *J. Biol. Chem. 279*, 23415−23421.
8. Geeves, M. A., Fedorov, R., and Manstein, D. J. (2005) Molecular mechanism of actomyosin-based motility, *Cell Mol. Life Sci. 62*, 1462−1477.
9. Coureux, P. D., Wells, A. L., Menetrey, J., Yengo, C. M., Morris, C. A., Sweeney, H. L., and Houdusse, A. (2003) A structural state of the myosin V motor without bound nucleotide, *Nature 425*, 419−423.
10. Holmes, K. C., Schroder, R. R., Sweeney, H. L., and Houdusse, A. (2004) The structure of the rigor complex and its implications for the power stroke, *Philos. Trans. R. Soc. London, B: Biol. Sci. 359*, 1819−1828.
11. Root, D. D., Stewart, S., and Xu, J. (2002) Dynamic docking of myosin and actin observed with resonance energy transfer, *Biochemistry 41*, 1786−1794.
12. Shestakov, D. A., and Tsaturian, A. K. (2006) [Refining the structure of the strongly bound actin-myosin complex by protein docking], *Biofizika 51*, 57−64.
13. Holmes, K. C., Angert, I., Kull, F. J., Jahn, W., and Schroder, R. R. (2003) Electron cryo-microscopy shows how strong binding of myosin to actin releases nucleotide, *Nature 425*, 423−427.
14. Malnasi-Csizmadia, A., Woolley, R. J., and Bagshaw, C. R. (2000) Resolution of conformational states of Dictyostelium myosin II motor domain using tryptophan (W501) mutants: implications for the open-closed transition identified by crystallography, *Biochemistry 39*, 16135−16146.
15. Malnasi-Csizmadia, A., Pearson, D. S., Kovacs, M., Woolley, R. J., Geeves, M. A., and Bagshaw, C. R. (2001) Kinetic resolution of a conformational transition and the ATP hydrolysis step using relaxation methods with a Dictyostelium myosin II mutant containing a single tryptophan residue, *Biochemistry 40*, 12727−12737.
16. Bagshaw, C. R., and Trentham, D. R. (1974) The characterization of myosin-product complexes and of product-release steps during the magnesium ion-dependent adenosine triphosphatase reaction, *Biochem. J. 141*, 331−349.
17. Manstein, D. J., and Hunt, D. M. (1995) Overexpression of myosin motor domains in Dictyostelium: screening of transformants and purification of the affinity tagged protein, *J. Muscle Res. Cell Motil. 16*, 325−332.
18. Pardee, J. D., and Spudich, J. A. (1982) Purification of muscle actin, *Methods Cell Biol. 24*, 271−289.
19. Spudich, J. A., and Watt, S. (1971) The regulation of rabbit skeletal muscle contraction. I. Biochemical studies of the interaction of the tropomyosin-troponin complex with actin and the proteolytic fragments of myosin, *J. Biol. Chem. 246*, 4866−4871.
20. Cooper, J. A., Walker, S. B., and Pollard, T. D. (1983) Pyrene actin: documentation of the validity of a sensitive assay for actin polymerization, *J. Muscle Res. Cell Motil. 4*, 253−262.
21. Kintses, B., Simon, Z., Gyimesi, M., Toth, J., Jelinek, B., Niedetzky, C., Kovacs, M., and Malnasi-Csizmadia, A. (2006) Enzyme kinetics above denaturation temperature: a temperature-jump/stopped-flow apparatus, *Biophys. J. 91*, 4605−4610.
22. Conibear, P. B., Malnasi-Csizmadia, A., and Bagshaw, C. R. (2004) The effect of F-actin on the relay helix position of myosin II, as revealed by tryptophan fluorescence, and its implications for mechanochemical coupling, *Biochemistry 43*, 15404−15417.
23. Kovacs, M., Malnasi-Csizmadia, A., Woolley, R. J., and Bagshaw, C. R. (2002) Analysis of nucleotide binding to Dictyostelium myosin II motor domains containing a single tryptophan near the active site, *J. Biol. Chem. 277*, 28459−28467.
24. Sellers, J. R. (1999) *Myosins*, Oxford University Press, New York.
25. White, H. D., Belknap, B., and Webb, M. R. (1997) Kinetics of nucleoside triphosphate cleavage and phosphate release steps by associated rabbit skeletal actomyosin, measured using a novel fluorescent probe for phosphate, *Biochemistry 36*, 11828−11836.
26. Giese, K. C., and Spudich, J. A. (1997) Phenotypically selected mutations in myosin's actin binding domain demonstrate intermolecular contacts important for motor function, *Biochemistry 36*, 8465−8473.
27. Nyitrai, M., and Geeves, M. A. (2004) Adenosine diphosphate and strain sensitivity in myosin motors, *Philos. Trans. R. Soc. London, B: Biol. Sci. 359*, 1867−1877.
28. Fujita, H., Sugiura, S., Momomura, S., Omata, M., Sugi, H., and Sutoh, K. (1997) Characterization of mutant myosins of Dictyostelium discoideum equivalent to human familial hypertrophic cardiomyopathy mutants. Molecular force level of mutant myosins may have a prognostic implication, *J. Clin. Invest. 99*, 1010−1015.
29. Sweeney, H. L., Straceski, A. J., Leinwand, L. A., Tikunov, B. A., and Faust, L. (1994) Heterologous expression of a cardiomyopathic myosin that is defective in its actin interaction, *J. Biol. Chem. 269*, 1603−1605.
30. Sasaki, N., Asukagawa, H., Yasuda, R., Hiratsuka, T., and Sutoh, K. (1999) Deletion of the myopathy loop of Dictyostelium myosin II and its impact on motor functions, *J. Biol. Chem. 274*, 37840−37844.
31. Liu, X., Shu, S., Kovacs, M., and Korn, E. D. (2005) Biological, biochemical, and kinetic effects of mutations of the cardiomy-

opathy loop of Dictyostelium myosin II: importance of ALA400, *J. Biol. Chem. 280*, 26974−26983.
32. Sasaki, N., Ohkura, R., and Sutoh, K. (2002) Dictyostelium myosin II as a model to study the actin-myosin interactions during force generation, *J. Muscle Res. Cell Motil. 23*, 697−702.
33. Joel, P. B., Trybus, K. M., and Sweeney, H. L. (2001) Two conserved lysines at the 50/20-kDa junction of myosin are necessary for triggering actin activation, *J. Biol. Chem. 276*, 2998−3003.
34. Joel, P. B., Sweeney, H. L., and Trybus, K. M. (2003) Addition of lysines to the 50/20 kDa junction of myosin strengthens weak binding to actin without affecting the maximum ATPase activity, *Biochemistry 42*, 9160−9166.
35. Furch, M., Geeves, M. A., and Manstein, D. J. (1998) Modulation of actin affinity and actomyosin adenosine triphosphatase by charge changes in the myosin motor domain, *Biochemistry 37*, 6317−6326.
36. Van, D. J., Furch, M., Lafont, C., Manstein, D. J., and Chaussepied, P. (1999) Functional characterization of the secondary actin binding site of myosin II, *Biochemistry 38*, 15078−15085.
37. Sasaki, N., Ohkura, R., and Sutoh, K. (2000) Insertion or deletion of a single residue in the strut sequence of Dictyostelium myosin II abolishes strong binding to actin, *J. Biol. Chem. 275*, 38705−38709.
38. Fujita-Becker, S., Reubold, T. F., and Holmes, K. C. (2006) The actin-binding cleft: functional characterisation of myosin II with a strut mutation, *J. Muscle Res. Cell Motil. 27*, 115−123.
39. Sutoh, K., Ando, M., Sutoh, K., and Toyoshima, Y. Y. (1991) Site-directed mutations of Dictyostelium actin: disruption of a negative charge cluster at the N terminus, *Proc. Natl. Acad. Sci. U.S.A. 88*, 7711−7714.
40. Cook, R. K., Root, D., Miller, C., Reisler, E., and Rubenstein, P. A. (1993) Enhanced stimulation of myosin subfragment 1 ATPase activity by addition of negatively charged residues to the yeast actin NH2 terminus, *J. Biol. Chem. 268*, 2410−2415.
41. Miller, C. J., Cheung, P., White, P., and Reisler, E. (1995) Actin's view of actomyosin interface, *Biophys. J. 68*, 50S-54S.
42. Miller, C. J., and Reisler, E. (1995) Role of charged amino acid pairs in subdomain-1 of actin in interactions with myosin, *Biochemistry 34*, 2694−2700.
43. Johara, M., Toyoshima, Y. Y., Ishijima, A., Kojima, H., Yanagida, T., and Sutoh, K. (1993) Charge-reversion mutagenesis of Dictyostelium actin to map the surface recognized by myosin during ATP-driven sliding motion, *Proc. Natl. Acad. Sci. U.S.A. 90*, 2127−2131.
44. Razzaq, A., Schmitz, S., Veigel, C., Molloy, J. E., Geeves, M. A., and Sparrow, J. C. (1999) Actin residue glu(93) is identified as an amino acid affecting myosin binding, *J. Biol. Chem. 274*, 28321−28328.
45. Schwyter, D. H., Kron, S. J., Toyoshima, Y. Y., Spudich, J. A., and Reisler, E. (1990) Subtilisin cleavage of actin inhibits in vitro sliding movement of actin filaments over myosin, *J. Cell Biol. 111*, 465−470.

BI701554A